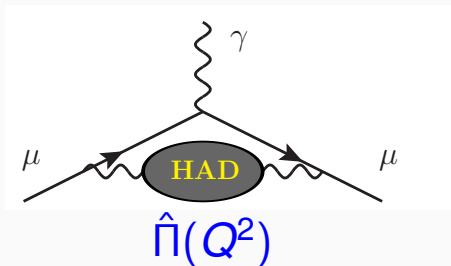


Review on Lattice Muon $g-2$ HVP Calculation

Kohtaroh Miura
(GSI Helmholtz-Institute Mainz)

**Lattice 2018, 36th International Symposium on Lattice Field Theory,
Michigan State University USA, 22 – 28 July 2018**

Hadron Vacuum Polarization (HVP) Contribution to Muon $g - 2$



$a_{\mu}^{exp.}$ vs. a_{μ}^{SM}

SM contribution	$a_{\mu}^{contrib.} \times 10^{10}$	Ref.
QED [5 loops]	11658471.8951 ± 0.0080	[Aoyama et al '12]
HVP-LO (pheno.)	692.6 ± 3.3	[Davier et al '16]
	694.9 ± 4.3	[Hagiwara et al '11]
	681.5 ± 4.2	[Benayoun et al '16]
	688.8 ± 3.4	[Jegerlehner '17]
HVP-NLO (pheno.)	-9.84 ± 0.07	[Hagiwara et al '11]
		[Kurz et al '11]
HVP-NNLO	1.24 ± 0.01	[Kurz et al '11]
HLbyL	10.5 ± 2.6	[Prades et al '09]
Weak (2 loops)	15.36 ± 0.10	[Gnendiger et al '13]
SM tot [0.42 ppm]	11659180.2 ± 4.9	[Davier et al '11]
[0.43 ppm]	11659182.8 ± 5.0	[Hagiwara et al '11]
[0.51 ppm]	11659184.0 ± 5.9	[Aoyama et al '12]
Exp [0.54 ppm]	11659208.9 ± 6.3	[Bennett et al '06]
Exp – SM	28.7 ± 8.0	[Davier et al '11]
	26.1 ± 7.8	[Hagiwara et al '11]
	24.9 ± 8.7	[Aoyama et al '12]

$a_{\mu}^{LO-HVP|NoNewPhys} \times 10^{10} \simeq 720 \pm 7,$
 FNAL E989 (2017): 0.14-ppm, J-PARC E34: 0.1-ppm

Really $a_{\mu}^{exp.} \neq a_{\mu}^{SM}$?

Motivation

HVP in Phenomenology

- The HVP in Pheno. is:

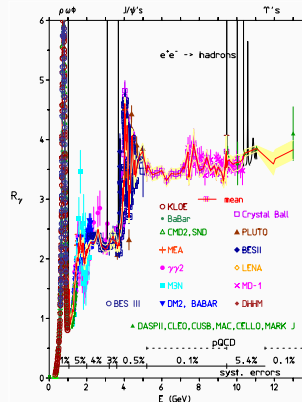
$$\hat{\Pi}(Q^2) = \int_0^\infty ds \frac{Q^2}{s(s+Q^2)} \frac{\text{Im}\Pi(s)}{\pi}$$

$$= (Q^2/(12\pi^2)) \int_0^\infty ds \frac{R_{had}(s)}{s(s+Q^2)},$$

- with R-ratio [right fig. Jegerlehner EPJ-Web2016] given by

$$R_{had}(s) \equiv \frac{\sigma(e^+e^- \rightarrow had.)}{4\pi\alpha^2(s)/(3s)},$$

- where the systematics is challenging to control(next talk). Some tension among experiments in $\sigma(e^+e^- \rightarrow \pi^+\pi^-)$.



Requirement for Lattice QCD:

- Independent cross-check of Hadronic Vacuum Polarization Contribution to muon g-2 (a_μ^{HVP}),
- Permil-Level determination of a_μ^{HVP} w.r.t. FNAL/J-PARC expr.

Motivation

HVP in Phenomenology

- The HVP in Pheno. is:

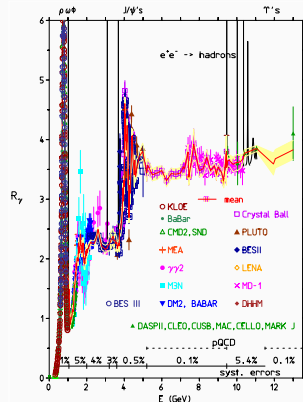
$$\hat{\Pi}(Q^2) = \int_0^\infty ds \frac{Q^2}{s(s+Q^2)} \frac{\text{Im}\Pi(s)}{\pi}$$

$$= (Q^2/(12\pi^2)) \int_0^\infty ds \frac{R_{had}(s)}{s(s+Q^2)},$$

- with R-ratio [right fig. Jegerlehner EPJ-Web2016] given by

$$R_{had}(s) \equiv \frac{\sigma(e^+e^- \rightarrow had.)}{4\pi\alpha^2(s)/(3s)},$$

- where the systematics is challenging to control(next talk). Some tension among experiments in $\sigma(e^+e^- \rightarrow \pi^+\pi^-)$.



Requirement for Lattice QCD:

- Independent cross-check of Hadronic Vacuum Polarization Contribution to muon $g-2$ (a_μ^{HVP}),
- Permil-Level determination of a_μ^{HVP} w.r.t. FNAL/J-PARC expr.

Objective in This Work

● Hadron Vacuum Polarization (HVP):

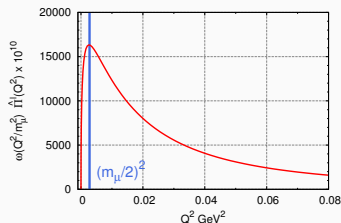
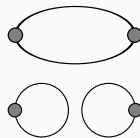
$$\begin{aligned}\Pi_{\mu\nu}(Q) &= \int d^4x \, e^{iQx} \langle j_\mu(x) j_\nu(0) \rangle \\ &= (Q_\mu Q_\nu - \delta_{\mu\nu} Q^2) \Pi(Q^2), \\ j_\mu &= \frac{2}{3} \bar{u} \gamma_\mu u - \frac{1}{3} \bar{d} \gamma_\mu d - \frac{1}{3} \bar{s} \gamma_\mu s + \frac{2}{3} \bar{c} \gamma_\mu c + \dots.\end{aligned}$$

● Leading-Order(LO) HVP Contr. to Muon g-2:

$$\begin{aligned}a_\mu^{\text{LO-HVP}} &= (\alpha/\pi)^2 \int_0^\infty dQ^2 \, \omega(Q^2/m_\mu^2) \hat{\Pi}(Q^2), \\ \hat{\Pi}(Q^2) &= \Pi(Q^2) - \Pi(0).\end{aligned}$$

● HVP Time-Moments:

$$\begin{aligned}\hat{\Pi}(Q^2) &= \sum_{n=1} Q^{2n} \Pi_n, \\ \Pi_n &= \frac{1}{n!} \left. \frac{d^n \hat{\Pi}(Q^2)}{(dQ^2)^n} \right|_{Q^2 \rightarrow 0} = \sum_x \frac{(-\hat{x}_\nu^2)^{n+1}}{(2n+2)!} \langle j_\mu(x) j_\mu(0) \rangle.\end{aligned}$$



Access to Deep IR: Pade and Time-Moment Rep.

Model Independent Approximants

Pade Approximant

- For $Q^2 < Q_{cut}^2$, lattice HVP data are fitted to

$$\hat{\Pi}(Q^2) = \frac{A_2 Q^2 + \dots}{1 + B_2 Q^2 + \dots} . \quad (1)$$

- The dispersion relation $\hat{\Pi}(Q^2) = \int_0^\infty ds \frac{Q^2}{s(s+Q^2)} \frac{\text{Im}\Pi(s)}{\pi}$ is seen as so-called *Stieltjes Integral* [Aubin et.al., PRD2012], which guarantees a finite conversion radius.

Time-Momentum Representation (TMR)

- For $Q^2 < Q_{uv-cut}^2$, define [Bernecker and Meyera, EPJA2011],

$$\hat{\Pi}(Q^2) = \sum_t t^2 \left[1 - \left(\frac{\sin[Qt/2]}{Qt/2} \right)^2 \right] \frac{1}{3} \sum_{i=1}^3 \langle j_i(t) j_i(0) \rangle . \quad (2)$$

- The momentum Q is *Continuous*. The Sine-Cardinal $\sin[Qt/2]/(Qt/2)$ accounts for a periodic feature of lattice correlators $\langle j_i(t) j_i(0) \rangle$.

Access to Deep IR: Pade and Time-Moment Rep.

Model Independent Approximants

Pade Approximant

- For $Q^2 < Q_{cut}^2$, lattice HVP data are fitted to

$$\hat{\Pi}(Q^2) = \frac{A_2 Q^2 + \dots}{1 + B_2 Q^2 + \dots} . \quad (1)$$

- The dispersion relation $\hat{\Pi}(Q^2) = \int_0^\infty ds \frac{Q^2}{s(s+Q^2)} \frac{\text{Im}\Pi(s)}{\pi}$ is seen as so-called *Stieltjes Integral* [Aubin et.al., PRD2012], which guarantees a finite conversion radius.

Time-Momentum Representation (TMR)

- For $Q^2 < Q_{uv-cut}^2$, define [Bernecker and Meyera, EPJA2011],

$$\hat{\Pi}(Q^2) = \sum_t t^2 \left[1 - \left(\frac{\sin[Qt/2]}{Qt/2} \right)^2 \right] \frac{1}{3} \sum_{i=1}^3 \langle j_i(t) j_i(0) \rangle . \quad (2)$$

- The momentum Q is *Continuous*. The Sine-Cardinal $\sin[Qt/2]/(Qt/2)$ accounts for a periodic feature of lattice correlators $\langle j_i(t) j_i(0) \rangle$.

Example of TMR

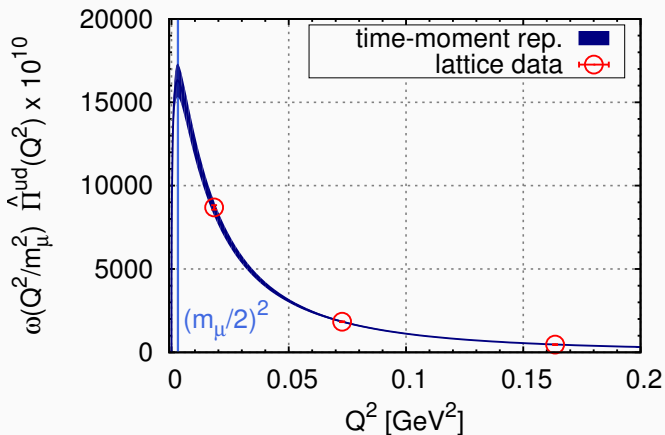


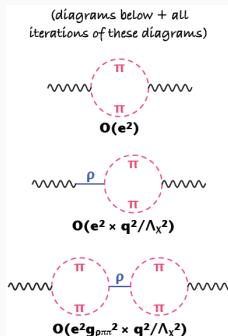
Figure: From BMW Ensemble ($a = 0.064$ fm) used in PRD2017 and PRL2018.

Table of Contents

- 1 Introduction
- 2 Challenges and Progresses
 - Large Distance Systematics
 - Continuum Extrapolation
 - SIB/QED Corrections
- 3 Discussion
 - Comparisons
 - Lattice QCD Combined with Phenomenology
- 4 Summary and Conclusions

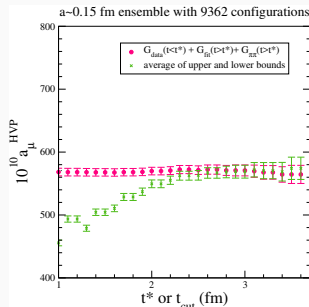
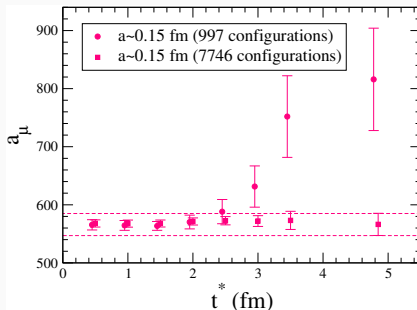
Table of Contents

- 1 Introduction
- 2 Challenges and Progresses
 - Large Distance Systematics
 - Continuum Extrapolation
 - SIB/QED Corrections
- 3 Discussion
 - Comparisons
 - Lattice QCD Combined with Phenomenology
- 4 Summary and Conclusions



- ◀ ◻ ▶ ◀ ◻ ▶ ◀ ≡ ▶ ◀ ≡ ▶ ≡|≡ ↺ 🔍 ↻

Multi-Exponential Fits [FNAL/HPQCD/MILC Preliminary]



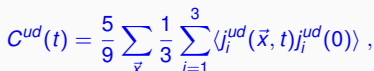
- **Left:** The t^* dependence of

$$a_{\mu,ud}^{\text{LO-HVP}}(t^*) = \left(\frac{\alpha}{\pi}\right)^2 \int_0^\infty dQ^2 \, \omega(Q^2/m_\mu^2) \, \mathcal{FT}[G^{ud}(t, t^*), Q^2]_{\text{with } P_{\text{ade}}} . \quad (3)$$

With high-statistics, $a_{\mu,ud}^{\text{LO-HVP}}$ get stable at larger t^* . For $t^* \lesssim 2 \text{ fm}$, low-(used in PRD2017) and high-statistics are consistent.

- **Right:** The high-statistics in the left-panel is compared with *Bounding Method* (next page).

Figure shows



- The connected-light correlator $C^{ud}(t)$ loses signal for $t > 3fm$. To control statistical error, consider $C^{ud}(t > t_c) \rightarrow C^{ud}_{up/low}(t, t_c)$, where

$$C_{\text{low}}^{ud}(t, t_c) = 0.0,$$

and $E_{2\pi} = 2(M_\pi^2 + (2\pi/L)^2)^{1/2}$.

- Similarly, $C^{disc}(t) \rightarrow C_{up/low}^{disc}(t, t_c)$,

$$-C_{\text{up}}^{\text{disc}}(t > t_c) = 0.1 C_{\text{ud}}^{\text{ud}}(t_c) \varphi(t)/\varphi(t_c),$$

$$-C_{\text{low}}^{\text{disc}}(t > t_c) = 0.0.$$

- By construction,

$$C_{low}^{ud, disc}(t, \mathbf{t}_c) \leq C^{ud, disc}(t) \leq C_{up}^{ud, disc}(t, \mathbf{t}_c).$$

Bounding [BMW PRL2018]

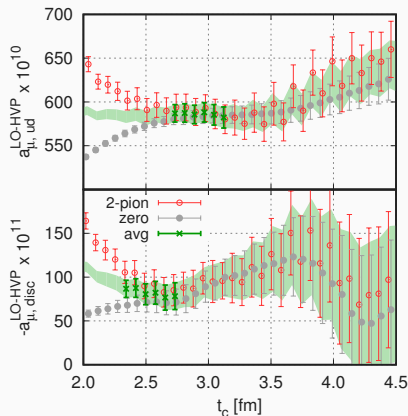


Figure: BMW, PRL2018.

- Corresponding to $C_{up/low}^{ud,disc}(t_c)$, we obtain upper/lower bounds for $\mu_{\text{on g-2}}$:
 $a_{\mu, up/low}^{ud,disc}(t_c)$.
- Two bounds meet around $t_c = 3fm$. Consider the average of bounds:
 $\bar{a}_{\mu}^{ud,disc}(t_c) = 0.5(a_{\mu, up}^{ud,disc} + a_{\mu, low}^{ud,disc})(t_c)$,
 which is stable around $t_c = 3fm$.
- We pick up such averages $\bar{a}_{\mu}^{ud,disc}(t_c)$ with 4 – 6 kinds of t_c around $3fm$. The average of average is adopted as $a_{\mu, ud/disc}^{LO-HVP}$ to be analysed, and a fluctuation over selected t_c gives systematic error.
- A similar method is proposed by C. Lehner in Lattice2016 and used in RBC/UKQCD-PRL2018. Improved bounding method with GEVP:
 [A. Meyer/C. Lehner, 27 Fri Hadron Structure].

Large Distance Control Using F_π , [Mainz CLS JHEP2017]

● Isospin Decomp. of Vector-Current Correlator:

$$G(t, L) = G^{I=1}(t, L) + G^{I=0}(t, L), \quad G^{I=1}(t, L) = \sum_{n=1} |A_n|^2 e^{-\omega_n t}, \quad (4)$$

where $\omega_n = 2\sqrt{M_\pi^2 + k_n^2}$. Investigate the large distance behavior of $G^{I=1}(t)$.

● Lüscher's Formula [NPB1991]: The p-wave phase shift determines k_n ,

$$\delta_{I=1}(k_n) + \phi(k_n L / (2\pi)) = n\pi, \quad (5)$$

where ϕ is a known kinematical function.

● Meyer's Formula [PRL2011]:

$$|F_\pi(\omega_n)|^2 = \frac{3\pi\omega_n^2}{2k_n^5} \left(k_n \frac{\partial \delta_1(k_n)}{\partial k_n} + q_n \frac{\partial \phi(q_n)}{\partial q_n} \right) |A_n|^2, \quad q_n = \frac{k_n L}{2\pi}, \quad (6)$$

which is analogous to Lellouch-Lüscher Formula [CMP2012].

● Gounaris-Sakurai(GS) [PRL1968] (c.f. Fransis et.al. [PRD2013]):

$$(k^3/\omega) \cot \delta_1^{\text{GS}}(k) = k^2 h(\omega) - k_\rho^2 h(M_\rho) + b[k_\rho, M_\rho, \Gamma_\rho](k^2 - k_\rho^2),$$

$$F_\pi^{\text{GS}}(\omega) = f_0[M_\pi, M_\rho, \Gamma_\rho] / ((k^3/\omega)(\cot[\delta_1^{\text{GS}}(k)] - i)), \quad k_\rho^2 = (M_\rho^2/4) - M_\pi^2.$$

● Construct $G^{I=1}(t)$: For given lattice data $(M_{\pi,\rho})$, using GS formulae with Eqs. (5) and (6), $G_{\text{lat}}^{I=1}(t)$ is fitted to Eq. (4) to determine (A_n, k_n, Γ_ρ) .

Large Distance Control Using F_π , [Mainz CLS JHEP2017]

● Isospin Decomp. of Vector-Current Correlator:

$$G(t, L) = G^{I=1}(t, L) + G^{I=0}(t, L), \quad G^{I=1}(t, L) = \sum_{n=1} |A_n|^2 e^{-\omega_n t}, \quad (4)$$

where $\omega_n = 2\sqrt{M_\pi^2 + k_n^2}$. Investigate the large distance behavior of $G^{I=1}(t)$.

● Lüscher's Formula [NPB1991]: The p-wave phase shift determines k_n ,

$$\delta_{I=1}(k_n) + \phi(k_n L / (2\pi)) = n\pi, \quad (5)$$

where ϕ is a known kinematical function.

● Meyer's Formula [PRL2011]:

$$|F_\pi(\omega_n)|^2 = \frac{3\pi\omega_n^2}{2k_n^5} \left(k_n \frac{\partial \delta_1(k_n)}{\partial k_n} + q_n \frac{\partial \phi(q_n)}{\partial q_n} \right) |A_n|^2, \quad q_n = \frac{k_n L}{2\pi}, \quad (6)$$

which is analogous to Lellouch-Lüscher Formula [CMP2012].

● Gounaris-Sakurai(GS) [PRL1968] (c.f. Fransis et.al. [PRD2013]):

$$(k^3/\omega) \cot \delta_1^{\text{GS}}(k) = k^2 h(\omega) - k_\rho^2 h(M_\rho) + b[k_\rho, M_\rho, \Gamma_\rho](k^2 - k_\rho^2),$$

$$F_\pi^{\text{GS}}(\omega) = f_0[M_\pi, M_\rho, \Gamma_\rho] / ((k^3/\omega)(\cot[\delta_1^{\text{GS}}(k)] - i)), \quad k_\rho^2 = (M_\rho^2/4) - M_\pi^2.$$

● Construct $G^{I=1}(t)$: For given lattice data $(M_{\pi,\rho})$, using GS formulae with Eqs. (5) and (6), $G_{\text{lat}}^{I=1}(t)$ is fitted to Eq. (4) to determine (A_n, k_n, Γ_ρ) .

Large Distance Control Using F_π , [Mainz CLS JHEP2017]

● Isospin Decomp. of Vector-Current Correlator:

$$G(t, L) = G^{I=1}(t, L) + G^{I=0}(t, L), \quad G^{I=1}(t, L) = \sum_{n=1} |A_n|^2 e^{-\omega_n t}, \quad (4)$$

where $\omega_n = 2\sqrt{M_\pi^2 + k_n^2}$. Investigate the large distance behavior of $G^{I=1}(t)$.

● Lüscher's Formula [NPB1991]: The p-wave phase shift determines k_n ,

$$\delta_{I=1}(k_n) + \phi(k_n L / (2\pi)) = n\pi, \quad (5)$$

where ϕ is a known kinematical function.

● Meyer's Formula [PRL2011]:

$$|F_\pi(\omega_n)|^2 = \frac{3\pi\omega_n^2}{2k_n^5} \left(k_n \frac{\partial \delta_1(k_n)}{\partial k_n} + q_n \frac{\partial \phi(q_n)}{\partial q_n} \right) |A_n|^2, \quad q_n = \frac{k_n L}{2\pi}, \quad (6)$$

which is analogous to Lellouch-Lüscher Formula [CMP2012].

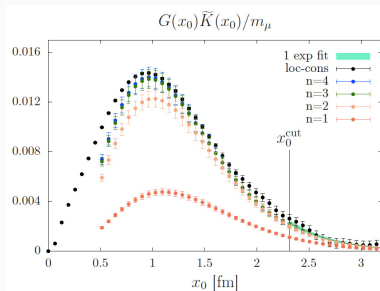
● Gounaris-Sakurai(GS) [PRL1968] (c.f. Fransis et.al. [PRD2013]):

$$(k^3/\omega) \cot \delta_1^{\text{GS}}(k) = k^2 h(\omega) - k_\rho^2 h(M_\rho) + b[k_\rho, M_\rho, \Gamma_\rho](k^2 - k_\rho^2),$$

$$F_\pi^{\text{GS}}(\omega) = f_0[M_\pi, M_\rho, \Gamma_\rho] / ((k^3/\omega)(\cot[\delta_1^{\text{GS}}(k)] - i)), \quad k_\rho^2 = (M_\rho^2/4) - M_\pi^2.$$

● Construct $G^{I=1}(t)$: For given lattice data $(M_{\pi,\rho})$, using GS formulae with Eqs. (5) and (6), $G_{\text{lat}}^{I=1}(t)$ is fitted to Eq. (4) to determine (A_n, k_n, Γ_ρ) .

Large Distance Control Using F_π



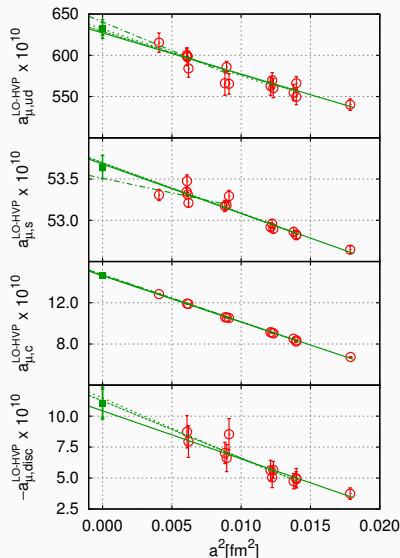
$$(A) \ G_n^{l=1}(t, L) = \sum_{j=1}^n |A_j|^2 e^{-\sqrt{M_\pi^2 + k_j^2} t},$$

$$(B) \ G_n^{l=1}(t > t^*, L \rightarrow \infty) = \frac{1}{48\pi^2} \int_{2M_\pi}^{\infty} d\omega \ \omega^2 \left(1 - \frac{4M_\pi^2}{\omega^2}\right)^{3/2} |F_\pi(\omega)|^2 e^{-\omega|t|}.$$

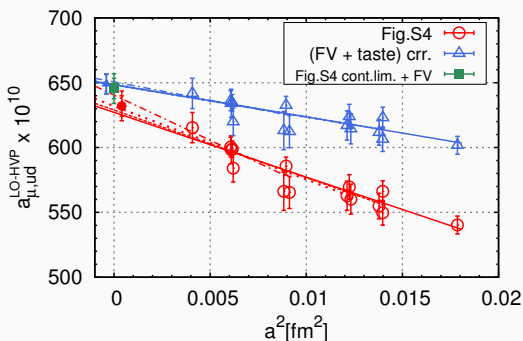
- Figure: [Mainz Prelim], update of [Mainz Lat2017]. $(\tilde{K}(t)/m_\mu)G_n(t, L)$ vs $x_0 = t$ for $N_f = 2 + 1$, $M_\pi = 200$ MeV. G_n is given by Eq. (A). c.f. Talk by H. Wittig (27 Fri, Hadron Structure).
- The lowest mode ($n = 1$) becomes dominant at around 3 [fm]. A single exponential-fit provides a good approximation at long-distance.
- Using $F_\pi^{\text{GS}}(\omega)$, the infinite-volume correlator $G_n^{l=1}(t, L \rightarrow \infty)$ is given by Eq. (B). Comparing $a_{\mu,ud}^{\text{LO-HVP}}$ obtained with $G_n^{l=1}(t > t^*, L \rightarrow \infty)$ or $G_{\text{lat}}^{l=1}(t > t^*, L)$, a finite volume effect can be estimated.

- $E_\rho = 0.766(21)$ [GeV]
(c.f. PDG: 0.77549(34) [GeV]).
- $\Gamma_\rho = 0.139(18)$ [GeV]
(c.f. PDG: 0.1462(7) [GeV]).

Continuum Extrapolation



Crosscheck of Continuum Extrapolation [BMW PRL2018]



- 1 Red open-circles are raw lattice data and continuum-extrapolated (red filled-circle). Then finite-volume correction using XPT is added to get the green-square point.
- 2 Similarly to HPQCD-PRD2017, raw data (red-circles) are first corrected with finite-volume and taste-partner effects to get blue open-triangles, which are continuum-extrapolated to get blue filled-triangle.

Continuum Extrapolation, Comparison

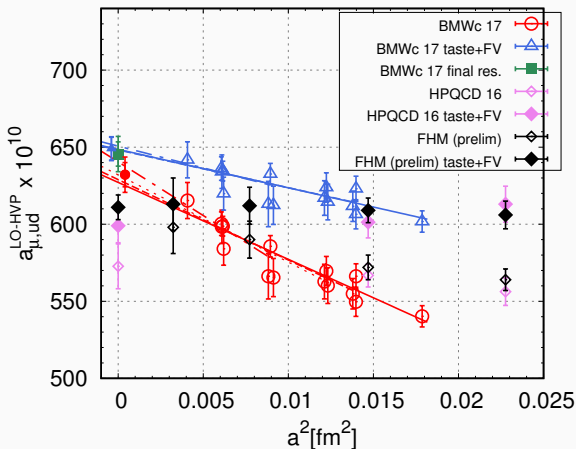


Figure: BMW-PRL2018 vs HPQCD-PRD2017 and FNAL/HPQCD/MILC-Prelim.

QED and Strong-Isospin Breaking Corrections

$$\mathcal{O}(\alpha) \sim \mathcal{O}\left(\frac{m_d - m_u}{\Lambda_{QCD}}\right) \sim 1\% \text{ Correction} .$$

Strong Isospin Breaking (SIB)

Strong isospin breaking: $m_d - m_u = 2.41(6)(4)(9)$ [BMW PRL2016] in \overline{MS} -2[GeV].

- Direct Simulations with $m_u \neq m_d$ [FNAL/HPQCD/MILC-PRL2018].

- Perturbative Method [RM123-JHEP2012,RBC/UKQCD-JHEP17]:

$$\begin{aligned}\langle O \rangle &= \langle O \rangle_{m_u/d=\hat{m}} + (m_{u/d} - \hat{m}) \frac{\partial \langle O \rangle}{\partial m_{u/d}} \Big|_{m_u=m_d} + \mathcal{O}((m_{u/d} - \hat{m})^2), \\ &= \langle O \rangle_{m_u/d=\hat{m}} - (m_{u/d} - \hat{m}) \langle OS \rangle_{m_u/d=\hat{m}},\end{aligned}$$

where $\hat{m} = (m_u + m_d)/2$, and $S = \sum_x \bar{q}_{u/d} q_{u/d}(x)$.



Up: Strong Isospin Breaking Diagrams.

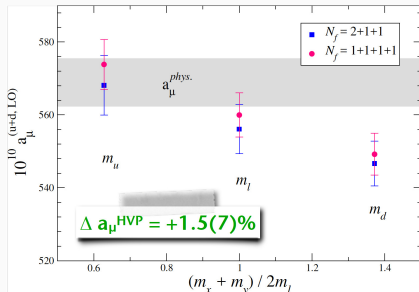
Right: FNAL/HPQCD/MILC-PRL2018 (Van de Water, Mainz g-2 workshop).

Valence-quark dep. of $a_\mu^{\text{LO-HVP}}$ for (2+1+1) and (1+1+1+1) ensemble. Two ensemble results agree at $m_l = (m_u + m_d)/2$;

sea-quark SIB are negligible. To quantify SIB, define, $\Delta a_\mu^{\text{LO-HVP}} =$

$$(4a_\mu^{\text{LO-HVP}}|_{m_u} + a_\mu^{\text{LO-HVP}}|_{m_d})/5 - a_\mu^{\text{LO-HVP}}|_{m_l}.$$

$$\text{SIB corr.} = \Delta a_\mu^{\text{LO-HVP}} / a_\mu^{\text{LO-HVP}}|_{m_l} = 1.5(7)\%$$



Strong Isospin Breaking (SIB)

Strong isospin breaking: $m_d - m_u = 2.41(6)(4)(9)$ [BMW PRL2016] in \overline{MS} -2[GeV].

- Direct Simulations with $m_u \neq m_d$ [FNAL/HPQCD/MILC-PRL2018].
- Perturbative Method [RM123-JHEP2012,RBC/UKQCD-JHEP17]:

$$\begin{aligned}\langle O \rangle &= \langle O \rangle_{m_u/d=\hat{m}} + (m_{u/d} - \hat{m}) \frac{\partial \langle O \rangle}{\partial m_{u/d}} \Big|_{m_u=m_d} + \mathcal{O}((m_{u/d} - \hat{m})^2), \\ &= \langle O \rangle_{m_u/d=\hat{m}} - (m_{u/d} - \hat{m}) \langle OS \rangle_{m_u/d=\hat{m}},\end{aligned}$$

where $\hat{m} = (m_u + m_d)/2$, and $S = \sum_x \bar{q}_{u/d} q_{u/d}(x)$.



Up: Strong Isospin Breaking Diagrams.

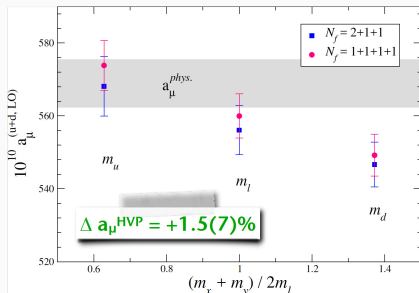
Right: FNAL/HPQCD/MILC-PRL2018 (Van de Water, Mainz g-2 workshop).

Valence-quark dep. of $a_\mu^{\text{LO-HVP}}$ for (2+1+1) and (1+1+1+1) ensemble. Two ensemble results agree at $m_l = (m_u + m_d)/2$;

sea-quark SIB are negligible. To quantify SIB, define, $\Delta a_\mu^{\text{LO-HVP}} =$

$$(4a_\mu^{\text{LO-HVP}}|_{m_u} + a_\mu^{\text{LO-HVP}}|_{m_d})/5 - a_\mu^{\text{LO-HVP}}|_{m_l}.$$

$$\text{SIB corr.} = \Delta a_\mu^{\text{LO-HVP}} / a_\mu^{\text{LO-HVP}}|_{m_l} = 1.5(7)\%$$



QED Correction

- Consider QCD + QED Euclidean partition function:

$$\langle O \rangle = \frac{1}{Z} \int \mathcal{D}[q, \bar{q}, U] \mathcal{D}[A] O e^{-S_F[q, \bar{q}, U, A] - S_G[U] e^{-S_\gamma[A]}} . \quad (7)$$

- Full QCD + QED:** First Come Out! [QCDSF-Prelim, talk by J. Zanotti (27 Fri, Hadron Structure)].
- Stochastic Method:** Stochastic photon fields A_μ are generated with weight e^{-S_γ} independently of gluon fields U_μ (electro-quenched), and multiplied, $U_\mu(x) \rightarrow e^{-ieq_f A_\mu(x)} U_\mu(x)$ [Duncan et.al. PRL1996].
- Perturbative Method:** QED can be treated in a perturbative way in $\alpha = e^2/(4\pi^2)$ [RM123-PRD2013]:

$$\langle O \rangle = \langle O \rangle_0 + \frac{e^2}{2} \frac{\partial^2 \langle O \rangle}{\partial e^2} \Big|_{e=0} + \mathcal{O}(\alpha^2) . \quad (8)$$

The stochastic and perturbative methods gave consistent corrections [RBC/UKQCD-Lat2017].

- To control QED FV effects, QED_L prescription [Hayakawa PTP2008] is used; spatial zero-modes and the universal $1/L^{n=1,2}$ corrections to mass are removed [BMW Science2015], while a reflection positivity is preserved.

QED Correction

- Consider QCD + QED Euclidean partition function:

$$\langle O \rangle = \frac{1}{Z} \int \mathcal{D}[q, \bar{q}, U] \mathcal{D}[A] O e^{-S_F[q, \bar{q}, U, A] - S_G[U] - S_\gamma[A]} . \quad (7)$$

- Full QCD + QED:** First Come Out! [QCDSF-Prelim, talk by J. Zanotti (27 Fri, Hadron Structure)].
- Stochastic Method:** Stochastic photon fields A_μ are generated with weight e^{-S_γ} independently of gluon fields U_μ (electro-quenched), and multiplied, $U_\mu(x) \rightarrow e^{-ieq_f A_\mu(x)} U_\mu(x)$ [Duncan et.al. PRL1996].
- Perturbative Method:** QED can be treated in a perturbative way in $\alpha = e^2/(4\pi^2)$ [RM123-PRD2013]:

$$\langle O \rangle = \langle O \rangle_0 + \frac{e^2}{2} \frac{\partial^2 \langle O \rangle}{\partial e^2} \Big|_{e=0} + \mathcal{O}(\alpha^2) . \quad (8)$$

The stochastic and perturbative methods gave consistent corrections [RBC/UKQCD-Lat2017].

- To control QED FV effects, QED_L prescription [Hayakawa PTP2008] is used; spatial zero-modes and the universal $1/L^{n-1,2}$ corrections to mass are removed [BMW Science2015], while a reflection positivity is preserved.

QED Correction

- Consider QCD + QED Euclidean partition function:

$$\langle O \rangle = \frac{1}{Z} \int \mathcal{D}[q, \bar{q}, U] \mathcal{D}[A] O e^{-S_F[q, \bar{q}, U, A] - S_G[U] - S_\gamma[A]} . \quad (7)$$

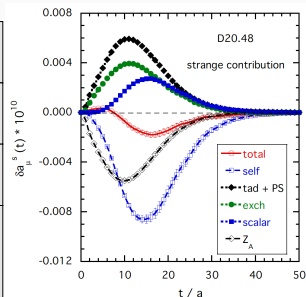
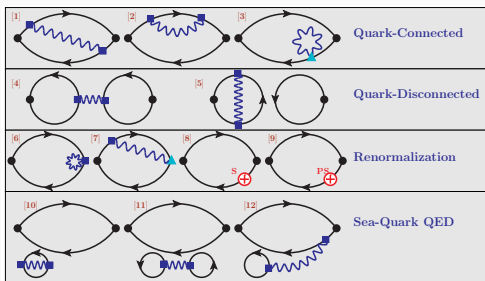
- Full QCD + QED:** First Come Out! [QCDSF-Prelim, talk by J. Zanotti (27 Fri, Hadron Structure)].
- Stochastic Method:** Stochastic photon fields A_μ are generated with weight e^{-S_γ} independently of gluon fields U_μ (electro-quenched), and multiplied, $U_\mu(x) \rightarrow e^{-ieq_f A_\mu(x)} U_\mu(x)$ [Duncan et.al. PRL1996].
- Perturbative Method:** QED can be treated in a perturbative way in $\alpha = e^2/(4\pi^2)$ [RM123-PRD2013]:

$$\langle O \rangle = \langle O \rangle_0 + \frac{e^2}{2} \frac{\partial^2 \langle O \rangle}{\partial e^2} \Big|_{e=0} + \mathcal{O}(\alpha^2) . \quad (8)$$

The stochastic and perturbative methods gave consistent corrections [RBC/UKQCD-Lat2017].

- To control QED FV effects, QED_L prescription [Hayakawa PTP2008] is used; spatial zero-modes and the universal $1/L^{n=1,2}$ corrections to mass are removed [BMW Science2015], while a reflection positivity is preserved.

QED Correction Diagrams in Perturbative Approach



- **Left:** ■ = vector-current, ▲ = tadpole, ⊕ = (pseudo)-scalar insertions.
- **Right:** [ETMc JHEP2017, talk by D. Giusti, (27 Fri, Hadron structure)] with corrections [1],[2],[3],[8] (mass retuning) and [9] (keeping maximal twist) for strange component.
- RBCUKQCD (Domain-Wall) considered [1],[2],[3],[4]; the others $\sim 1/N_c$ or irrelevant. One must take care of a double counting problem in [4] w.r.t. single-photon and additional gluons [talks by RBC/UKQCD (27 Fri, Hadron Structure).]
- For diagram details, see [talk by A. Risch (24 Tue, Hadron Spectroscopy)].

SIB + QED Corrections, Short Summary

- **ETMc Preliminary**

$$\delta a_{\mu}^{\text{LO-HVP}} \times 10^{10} = 7(2) \text{ (quark connected and qQED).}$$

- **BMW PRL2018**

$$\delta a_{\mu}^{\text{LO-HVP}} \times 10^{10} = 7.8(5.1) \text{ (pheno. } (\pi^0\gamma, \eta\gamma, \rho - \omega \text{ mix, } M_{\pi\pm})).$$

- **RBC/UKQCD PRL2018**

$$\delta a_{\mu}^{\text{LO-HVP}} \times 10^{10} = 9.5(10.2) \text{ (quark connected + one disconnected and qQED. Also relevant to use tau decay input for HVP, [M. Bruno, 27 Fri Hadron Structure].)}$$

- **FNAL/HPQCD/MILC PRL2018**

$$\delta a_{\mu}^{\text{LO-HVP}} \times 10^{10} = 9.5(4.5) \text{ (Strong Isospin Breaking only).}$$

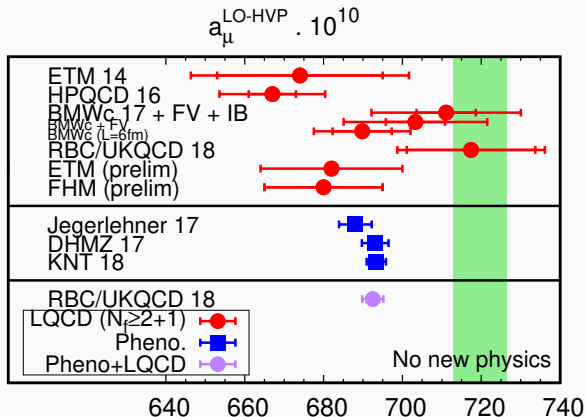
- **QCDSF Prelim:**

$$\delta a_{\mu}^{\text{LO-HVP}} / a_{\mu}^{\text{LO-HVP}} \lesssim 1\% \text{ (Dynamical QED, } M_{\pi} \sim 400[\text{MeV}] \text{)}$$

Table of Contents

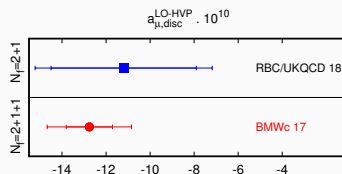
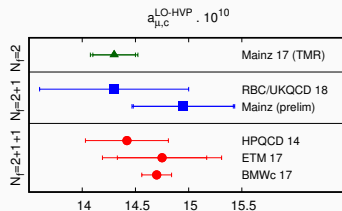
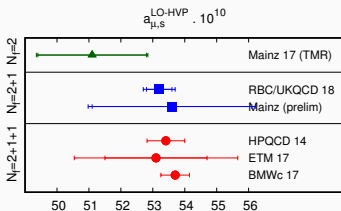
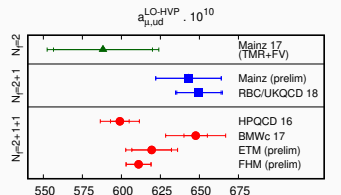
- 1 Introduction
- 2 Challenges and Progresses
 - Large Distance Systematics
 - Continuum Extrapolation
 - SIB/QED Corrections
- 3 Discussion
 - Comparisons
 - Lattice QCD Combined with Phenomenology
- 4 Summary and Conclusions

The obvious: $a_\mu^{\text{LO-HVP}}$



- Lattice errors $\sim 2\%$ vs phenomenology errors $\sim 0.4\%$.
- Some lattice results suggest new physics others not but all compatible with phenomenology.

$a_{\mu}^{\text{LO-HVP}}$: flavor by flavor comparison

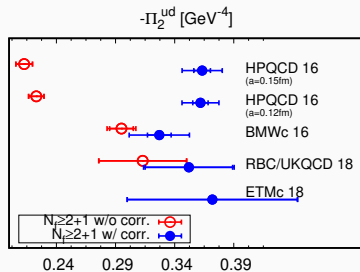
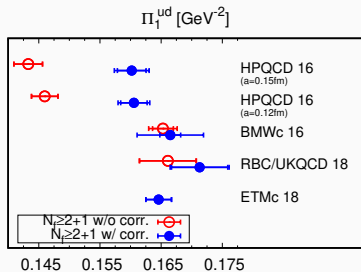


- $a_{\mu,s,c,disc}^{\text{LO-HVP}}$ already known with high enough precision for FNAL E989

- “Disagreement” is on $a_{\mu,ud}^{\text{LO-HVP}}$

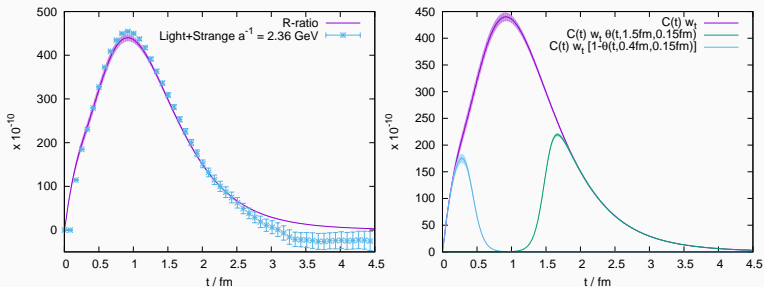
Derivatives of $\Pi(Q^2)$ at $Q^2 = 0$: ud contribution

$$\Pi_n = \frac{1}{n!} \frac{d^n \hat{\Pi}(Q^2)}{(dQ^2)^n} \Big|_{Q^2 \rightarrow 0} = \sum_x \frac{(-\hat{x}_\nu^2)^{n+1}}{(2n+2)!} \langle j_\mu(x) j_\mu(0) \rangle.$$



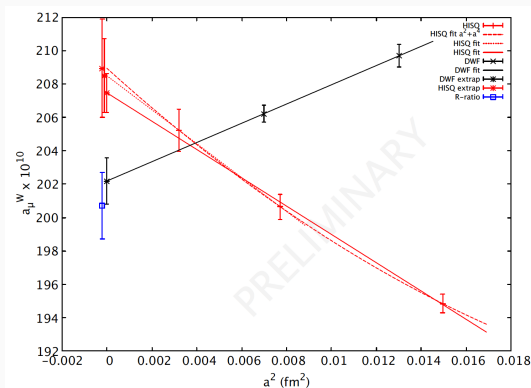
- In Pad picture, larger Π_1 (Π_2) \rightarrow larger (smaller) a_μ .
- HPQCD 16 has slightly smaller Π_1^{ud} and larger $-\Pi_2^{ud}$ than BMWc 16 and RBC/UKQCD 18 \rightarrow combine to give smaller $a_{\mu,ud}^{\text{LO-HVP}}$
- Suggests that HPQCD 16 has smaller $C(t)$ for $t \sim 1 \text{ fm}$ but larger for $t \gtrsim 2 \text{ fm}$
- Difference comes from HPQCD 16's large corrections

Time window: lattice + phenomenology



- Figure: [RBC/UKQCD-PRL2018, talk by C. Lehner and Colleagues (27 Fri, Hadron Structure)]. In $a_\mu^{\text{LO-HVP}} = (\alpha/\pi)^2 \sum_t W(t, Q^2/m_\mu^2) C(t)$, consider lattice/pheno correlators;
 $C_{\text{lat}}(t) = \sum_{\vec{x}} \frac{1}{3} \sum_{i=1}^3 \langle j_i(\vec{x}, t) j_i^{ud}(0) \rangle$, $C_{\text{pheno}}(t) = \frac{1}{2} \int_0^\infty ds \sqrt{s} \frac{R(s)}{3} e^{-\sqrt{s}|t|}$.
 $C_{\text{lat}}(t)$ may be more precise in intermediate $t \sim 1 \text{ [fm]}$.
- Consider the decomposition $C(t) = (C^{\text{SD}} + C^{\text{W}} + C^{\text{LD}})(t)$, where $(C^{\text{SD}}, C^{\text{W}}, C^{\text{LD}})(t) = C(t)(1 - \Theta(t, t_0, \Delta), \Theta(t, t_0, \Delta) - \Theta(t, t_1, \Delta), \Theta(t, t_1, \Delta))$ with the smeared step function, $\Theta(t, t', \Delta) = (1 + \tanh[(t - t')/\Delta])/2$.
- For $C^{\text{W}}(t)$, use lattice data $C_{\text{lat}}^{\text{W}}$. For the others, use phenomenological data $C_{\text{pheno}}^{\text{SD/LD}}$.
 $(t_0, t_1, \Delta) = (0.4, 1.0, 0.15)[\text{fm}]$, $a_\mu^{\text{LO-HVP}} = 692.5(2.7) \cdot 10^{-10}$ [RBC/UKQCD-PRL2018].

Window Method: DWF vs HISQ vs Pheno.



- Fig.: T. Blum (27 Fri). Continuum extrapolation of $a_\mu^W = \sum_t C_{lat}^W(t) W(t, m_\mu)$, where $C_{lat}^W(t) = C_{lat}(t)((\Theta(t, t_0, \Delta) - \Theta(t, t_1, \Delta)))$ with $t_0 = 4.0$, $t_1 = 1.0$, $\Delta = 0.15[\text{fm}]$.
- (2+1+1) HISQ(MILC ensemble) and DWF all physical points in 5.5 [fm] boxes. HISQ and DWF shows 2-3 σ tension; lattice spacing, statistics may be responsible. The DWF result is consistent with phenomenology.

Other Important Subjects

- Lattice ($Q^2 < Q_{cut}^2$) - Perturbation ($Q^2 \geq Q_{cut}^2$) Matching [BMW-PRL2018].
- Lattice results of Higher-Order HVP [FNAL/HPQCD/MILC, 1806.08190].
- Dual Propagator + Gounaris-Sakurai-Lüscher Propagator [ETMc-Prelim, Mainz g-2 Workshop].
- Omnès Formula for time-like pion form factor [Mainz Preliminary, talk by H. Wittig (27 Fri, Hadron Structure)].
- HVP for $\sin^2 \theta_W$ [talk by Cè Marco, (27 Fri, Hadron Structure)].

Table of Contents

- 1 Introduction
- 2 Challenges and Progresses
 - Large Distance Systematics
 - Continuum Extrapolation
 - SIB/QED Corrections
- 3 Discussion
 - Comparisons
 - Lattice QCD Combined with Phenomenology
- 4 Summary and Conclusions

Summary and Conclusions

- Lattice computation of $a_\mu^{\text{LO-HVP}}$ has total error $\sim 2\% \gg \sim 0.4\%$ from phenomenology. Some results are consistent with no new physics and phenomenology, others with phenomenology and new physics
- Difference comes from ud contribution and most probably from treatment of long-distance physics, for which many progress have been done but need more understandings.
- Comparison of ud time moments suggests:
 - larger intermediate-distance contribution in [BMWc-PRL2018 and RBC/UKQCD-PRL2018]
 - larger long-distance contribution in [HPQCD-PRD2017], associated with model description
- With current lattice results, too early to make detailed comparisons with dispersive approach. However, combination of lattice and phenomenology [RBC/UKQCD PRL18, T. Blum Preliminary] may deliver a reliable $0.2\% a_\mu^{\text{LO-HVP}}$.
- Lattice combined with Experimental Data: Next Talk by Marina.

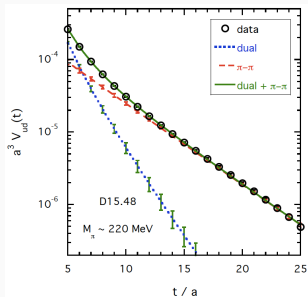
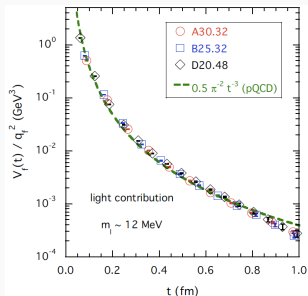
Summary and Conclusions

- Lattice computation of $a_\mu^{\text{LO-HVP}}$ has total error $\sim 2\% \gg \sim 0.4\%$ from phenomenology. Some results are consistent with no new physics and phenomenology, others with phenomenology and new physics
- Difference comes from ud contribution and most probably from treatment of long-distance physics, for which many progress have been done but need more understandings.
- Comparison of ud time moments suggests:
 - larger intermediate-distance contribution in [BMWc-PRL2018 and RBC/UKQCD-PRL2018]
 - larger long-distance contribution in [HPQCD-PRD2017], associated with model description
- With current lattice results, too early to make detailed comparisons with dispersive approach. However, combination of lattice and phenomenology [RBC/UKQCD PRL18, T. Blum Preliminary] may deliver a reliable $0.2\% a_\mu^{\text{LO-HVP}}$.
- Lattice combined with Experimental Data: Next Talk by Marina.

Table of Contents

5 Backups

Large Distance Control (GSL + SVZ) [ETMc Preliminary]



- Top panel [ETMc JHEP2017]: Vector-current correlator data are well described by 1-loop QCD up to $1\text{ fm} > \hbar c / \Lambda_{QCD}$. This was interpreted as the onset of SVZ Quark-Hadron Duality [NPB1979].

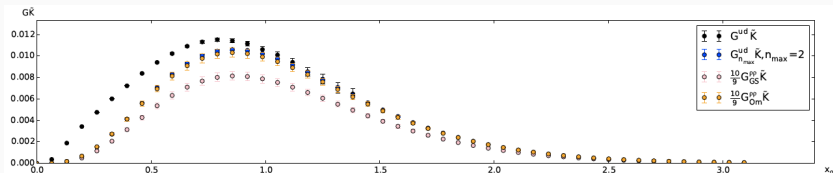
- Motivated by the duality, consider the following expression for the vector-current correlator,

$$V_{dual}(t) = \frac{5R_{dual}}{72\pi^2} \int_{s_{dual}}^{\infty} ds \sqrt{s} e^{-\sqrt{s}t} R^{1-QCD}(s),$$

$$\text{where, } R^{1-QCD}(s) = (1 - \frac{4m_{ud}^2}{s})^{1/2} (1 + \frac{2m_{ud}^2}{s}).$$

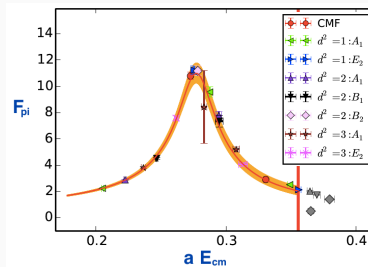
- This expression differs from 1-loop QCD by two fit params (R_{dual} , s_{dual}), and combined with 2-pion correlator $V_{\pi\pi}$ constructed via Gounaris-Sakurai F_{π}^{GS} .
- Bottom panel [ETMc Preliminary]: ($V_{dual} + V_{\pi\pi}$) describes well lattice data whole range. FV effects and other systematics can be studied with this.

Large Distance Control Omnès [Mainz Preliminary]

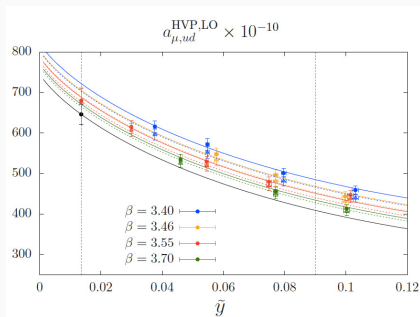
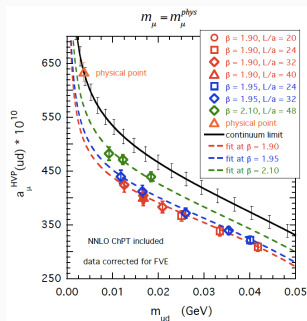


Omnès Formula (Nuovo Cimento (1958))

- Figs: Mainz Preliminary, Thanks to F.Erben (GSI-HIM).
- $F_\pi(\omega) = \exp \left[\omega^2 P_{n-1}(\omega^2) + \frac{\omega^{2n}}{\pi} \int_{4M_\pi^2}^{\infty} ds \frac{\delta_1(s)}{s^n(s-\omega^2-i\epsilon)} \right]$.
- Lattice data are used for F_π and δ_1 and fit parameters are in the Polynomial P_{n-1} .
- Omnès gives a better description than GS in the middle range.

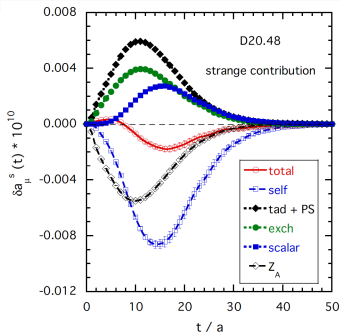
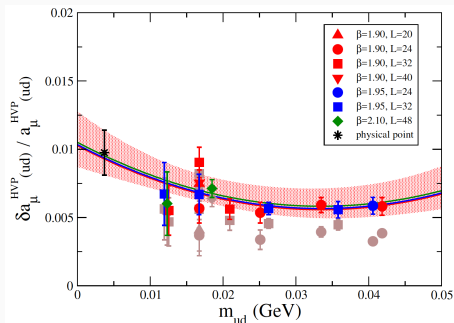


Continuum Extrapolation and Mass Dependence



- **Left:** ETM Preliminary. From slide by S.Simula in Mainz g-2 workshop 2018. The continuum limit line (black-solid) becomes sensitive to m_{ud} at physical point.
- **Right:** Mainz Preliminary. From slide by H.Meyer in Mainz g-2 workshop 2018. $\tilde{y} = (M_{\pi}/(4\pi f_{\pi}))^2$.

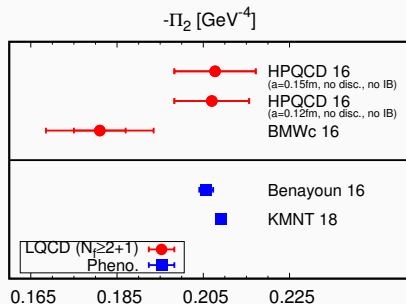
ISB + QED Corrections, [ETMc JHEP2017 and Preliminary]



- Left:** ETMc Preliminary, (SIB + QED) corrections for light components. The chiral/continuum-extrapolation is investigated with FV effects taken account.
- Right:** ETMc JHEP2017, (SIB + QED) corrections for strange component integrand for each diagrams shown previous pages. The charm is also investigated. In both, partial cancellations among the various diagrams.

Figure 1 shows the pion transition form factor $T_1^\pi(Q^2)$ as a function of Q^2 (GeV²). The plot includes data from several lattice QCD (LQCD) calculations and phenomenological (Pheno.) results. The x-axis is logarithmic, ranging from 0.096 to 0.104 GeV². The y-axis ranges from 0.0 to 0.025. The data points are as follows:

- HPQCD 16 (a=0.15fm, no disc., no IB): Red circle at $Q^2 \approx 0.097$ GeV², $T_1^\pi \approx 0.018$.
- HPQCD 16 (a=0.12fm, no disc., no IB): Red circle at $Q^2 \approx 0.098$ GeV², $T_1^\pi \approx 0.018$.
- BMWc 16: Red circle at $Q^2 \approx 0.101$ GeV², $T_1^\pi \approx 0.018$.
- Benayoun 16: Blue square at $Q^2 \approx 0.097$ GeV², $T_1^\pi \approx 0.012$.
- KMNT 18: Blue square at $Q^2 \approx 0.101$ GeV², $T_1^\pi \approx 0.012$.
- LQCD (N_f=2+1): Red circle at $Q^2 \approx 0.098$ GeV², $T_1^\pi \approx 0.018$.
- Pheno.: Blue square at $Q^2 \approx 0.097$ GeV², $T_1^\pi \approx 0.012$.



→ suggests that BMWc (and RBC/UKQCD) has $C(t)$ slightly larger for $t \sim 1$ fm and smaller for $t \gtrsim 2$ fm